Carbohydrate Polymers 155 (2017) 483–490

Contents lists available at ScienceDirect

Carbohydrate Polymers

journal homepage: www.elsevier.com/locate/carbpol

Impact of degree of oxidation on the physicochemical properties of microcrystalline cellulose

Jie Hao[a], Shuyi Xu[a], Naiyu Xu[a,*], Duxin Li[a], Robert J. Linhardt[b], Zhenqing Zhang[a,*]

[a] Jiangsu Key Laboratory of Translational Research and Therapy for Neuro-Psycho-Diseases and College of Pharmaceutical Sciences, Soochow University, Suzhou, Jiangsu 215021, China
[b] Center for Biotechnology and Interdisciplinary Studies, Rensselaer Polytechnic Institute, 110 8th St., Troy, NY, 12180, USA

ARTICLE INFO

Article history:
Received 2 August 2016
Received in revised form 27 August 2016
Accepted 4 September 2016
Available online 5 September 2016

Keywords:
Microcrystalline cellulose (MCC)
Degree of oxidation
Structure
Solubility
Oligosaccharide

ABSTRACT

Microcrystalline cellulose, a major component of cell wall of plants, is one of the most abundant natural materials, but the poor solubility of cellulose limits its applications. Cellulose is a linear glucan with exclusive β 1 → 4 linkage. Oxidation carried out with TEMPO–NaBr–NaClO system can selectively oxidize the C6 of glucose residues in cellulose. This modification improves polysaccharide solubility and other physicochemical properties. In this work, the impact of degree of oxidation on solubility, degree of crystallization, thermostability, molecular weight and the structures of the resulting oligosaccharide products of selectively oxidized cellulose were investigated using x-ray diffraction, thermogravimetric analysis, gel permeation chromatography–multiple angle laser light scattering and ultrahigh performance liquid chromatography–electrospray–quadrupole/time of flight–mass spectrometry, respectively. The physicochemical properties of selectively oxidized cellulose having different degrees of oxidation were carefully characterized providing a theoretical foundation for the more accurate selection of applications of oxidized celluloses.

1. Introduction

Microcrystalline cellulose (MCC), a linear glucan with exclusive β 1 → 4 linkage, is a major component of cell wall of plants (Klemm, Philip, Heinz, Heinz, & Wagenknecht, 1998; Li et al., 2015; Suhas et al., 2016). It is one of the most abundant natural materials. However, the pyknotic inter-molecular and intra-molecular hydrogen bonds in cellulose prevent most solvents from entering crystalline region and dissolving the cellulose (Bochek, Petropavlovsky, & Kallistov, 1993; Qin, Lu, Cai, & Zhang, 2013; Keshk, 2015). Concentrated alkaline solutions are one way to partially dissolve cellulose and include such solvents as concentrated aqueous NaOH and concentrated aqueous NaOH/urea solution (Qin, Lu, Cai, & Zhang, 2013; Keshk, 2015). This process of mercerization is used in limited areas, such as papermaking industry and production of macroporous cellulose membranes (Guo & Ruckenstein, 2002; Ruckenstein & Guo, 2001). Moreover, mercerized cellulose becomes insoluble again after the alkaline solution is removed, thus, this application of dissolving cellulose has limited utility.

Different derivatization reactions, such as carboxymethylation and oxidation have been used to improve the solubility and expand the application of cellulose (Kono, Oshima, Hashimoto, Shimizu, & Tajima, 2016; Isogai & Kato, 1998; Tahiri & Vignon, 2000). Carboxymethylated cellulose (CMC) is widely used in different areas, such as drug excipients (Ugwoke, Kaufmann, Verbeke, & Kinget, 2000). The degree of carboxymethylation affects both the solubility and viscosity of cellulose (Benchabane & Bekkour, 2008). Oxidation of cellulose improves polysaccharide solubility, viscosity and film-forming ability (Gomez-Bujedo, Fleury, & Vignon, 2004). Currently, there are two ways to produce oxidized cellulose, through specific and through nonspecific oxidation. Periodate is generally used for the nonspecific oxidation of cellulose (Jackson & Hudson, 1937; Sirvio, Hyvakko, Liimatainen, Niinimaki, & Hormi, 2011; Siller et al., 2015). In these reactions both the primary hydroxyl groups, at position 6, and the secondary hydroxyl groups at other positions on glucose (Glc) ring can be oxidized. The structures of these non-specifically oxidized products are always complicated. The better the structural characterization of an oxidized cellulose the more widely it can be used in different applications. The selective oxidation of cellulose with 2,2,6,6-tetramethylpiperidine-1-oxyl/sodium bromide/sodium hypochlorite (TEMPO – NaBr – NaClO) system has been recently reported (Isogai & Kato, 1998; Tahiri & Vignon, 2000; Gomez-Bujedo, Fleury, & Vignon, 2004; Shinoda, Saito, Okita, & Isogai, 2012; Benhamou, Dufresne, Magnin, Mortha, & Kaddami, 2014; Huang, Chen, Tsai, Hsieh, & Andrew Lin, 2015). In this selective oxidation, the primary hydroxyl groups at

* Corresponding authors.
E-mail address: z_zhang@suda.edu.cn (Z. Zhang).

http://dx.doi.org/10.1016/j.carbpol.2016.09.012
0144-8617/

carbon-6 are oxidized to afford glucuronic acid (GlcA) residues. This selective oxidation process provides the opportunity to produce oxidized cellulose having different properties under good quality control. This selectively oxidized cellulose, called cellulosic acid, has been used in the textile, cosmetic, and medical industries (Gomez-Bujedo, Fleury, & Vignon, 2004). However, all these applications of selectively oxidized cellulose were based on a limited understanding of their industrial properties. Unfortunately, the relationship between the degree of oxidation (DO) and the corresponding physicochemical properties has not been studied in detail.

In the current study, selectively oxidized celluloses having different DOs were prepared using a TEMPO–NaBr-NaClO system from mercerized microcrystalline cellulose (MCC). Their DOs were determined and compared using infrared spectroscopy (IR) and solid-state nuclear magnetic resonance (NMR) spectroscopy. The impact of DO on polysaccharide solubility, degree of crystallization, thermostability, molecular weight, and the structures of the resulting oligosaccharide products of oxidized MCC were investigated using x-ray diffraction (XRD), thermogravimetric analysis (TGA), and gel permeation chromatography–multiple angle laser light scattering (GPC-MALLS) and ultrahigh performance liquid chromatography–electrospray–quadrupole/time of flight–mass spectrometry (UHPLC-ESI-Q/TOF-MS), respectively. The physicochemical properties of selectively oxidized MCC with different DOs, carefully characterized by systematic analysis, represent an important foundation for more informed and accurate application of oxidized MCC for different uses.

2. Experimental

2.1. Materials

Commercial microcrystalline cellulose (MCC) was supplied by Sinopharm Chemical Reagent CO. Ltd. (Shanghai, China). Sodium hydroxide (NaOH) and concentrated hydrochloric acid (HCl) were both purchased from Chinasun Specialty Products CO., LTD. (Changshu, China). Sodium bromide (NaBr), 2,2,6,6-tetramethylpiperidine-1-oxyl (TEMPO) and sodium hypochlorite (NaClO, 5% active chlorine) were obtained from Aladdin Industrial Co. (Shanghai, China). Methanol (chromatographic grade) was obtained from Merck Chemicals (Darmstadt, Germany). Ammonium acetate (NH_4OAc, chromatographic grade) was supplied by Sigma-Aldrich (Shanghai, China). Deuteroxide (D_2O, atm.%D $\geq$ 99.9%) was purchased from Energy Chemicals (Shanghai, China). High-purity water (resistivity $\geq$ 18.2 M$\Omega \times$ cm, 25 °C) was used throughout the study. All other chemicals were of analytical reagents.

2.2. Methods

2.2.1. Procedure for oxidation of MCC with TEMPO mediated system

MCC, freshly mercerized with alkaline solution, improves its reactivity towards chemical modification (Guo & Ruckenstein, 2002; Ruckenstein & Guo, 2001; Assa, Belgacemb, & Frollinia, 2006; Gurgel, Melo, Lena, & Gil, 2009). All reactions in this work were carried out on MCC at a 1 g scale. MCC was freshly mercerized in 30 mL of 10% NaOH solution with magnetic stirring for 24 h before using. Each mercerized MCC solution was neutralized with 6 M HCl followed by desalting with 500 Da cut-off dialysis bag against DI water, which was afforded a volume of each reaction system of ~180 mL. After 32 mg TEMPO and 320 mg NaBr were added each reaction system was adjusted to pH 10 by the dropwise addition of 20% NaOH solution. Oxidations were carried out with different amounts of NaClO (1, 5, 10, 15 mL, 5% active chlorine) at 50 °C to afford oxidized MCC of various DOs. A pH meter was used to monitor the pH and 20% NaOH solution was used to maintain the pH at 10 during the reaction. Each reaction was terminated by adding 1 mL of ethanol after 4 h. The mixture was neutralized with 4 M HCl and dialyzed against DI water by using 500 Da molecular weight cut-off (MWCO) dialysis bag to eliminate TEMPO and other salts. The products remaining in the bag were concentrated with a rotary evaporator at 45 °C and then lyophilized. The oxidized MCC powders with different DOs were next ready to be analyzed.

2.2.2. Fourier transform infrared (FT-IR) spectroscopy

The FT-IR spectra of initial, mercerized, and oxidized MCCs (2 mg of each) were recorded using a FT-RI spectrometer (Vertex 70, Bruker, Germany) with the resolution of 4 cm^{-1}. The transmittance mode and 16 s scanning number were selected. The scanning was performed ranging from 4000 to 600 cm^{-1}. The data was processed and analyzed with OPUS.

2.2.3. NMR spectroscopic analysis

Solid-state ^{13}C NMR spectra of initial, mercerized, and oxidized MCCs were obtained on a WB/AVANCE III 400 MHz spectrometer (Bruker, Germany) with cross polarization and magic angle sample spinning. The spinning rate, pulse delay and contact time were set at 10 kHz, 3.5 s and 0.5 ms, respectively. The chemical shift was calibrated from an external standard of Adamantane. The NMR data was processed and analyzed using MestReNova.

2.2.4. X-ray diffraction (XRD) measurement

The XRD patterns of initial, mercerized, and oxidized MCCs (~30 mg of each) were performed on an X'Pert Pro MPD diffractometer (PANalytical B. V. Co., Netherlands). The X-ray source was Ni-filtered Cu Kα radiation at 40 kV and 30 mA and the 2θ range was set at 5 ~ 50°.

2.2.5. Thermogravimetric analysis (TGA)

The TG analysis of initial, mercerized and oxidized MCCs (~1 mg/each) were performed on a SDT 2960 thermal analyzer (TA Instruments, USA) under N_2 atmosphere. The heating rate was set at 10 °C/min and the scanning range was 20 ~ 490 °C.

2.2.6. Water solubility analysis

Water solubility of oxidized MCC is important for different applications (Keshk, 2015). Twenty milligrams of each sample was weighed out accurately (W) and dissolved in 4 mL distilled water before vigorous mixing on vortex mixer. The suspension was then centrifuged at 12000 rpm for 10 min. The supernatant was transferred out, lyophilized and weighed accurately (Ws). The solubility was calculated according to the following equation: Water solubility (%) = Ws/W $\times$ 100, where Ws is the mass of dissolved material in supernatant and W is the mass of total material (20 mg). The experiments were performed in triplicate.

2.2.7. Measurement of the molecular weight (MW) and distribution by GPC-MALLS

The weight-average MW of dissolved portion of each oxidized starch sample was determined by GPC-MALLS. In this experiment, an Agilent 1260 HPLC system (CA, USA) was coupled with an 18-angles MALLS (Wyatt, USA) and a refractive index (RI) detector (Agilent, USA). The dn/dc value was set at 0.138 mL/g. The separation was performed on an ACQUITY UPLC@BEH125 SEC column (1.7 μm, 4.6 $\times$ 300 mm, Waters, USA) at 0.1 mL/min and 25 °C. The mobile phase was 80 mM ammonium acetate aqueous solution. The injection volume was 20 μL solution. The data were processed with ASTRA software of version 6.1.

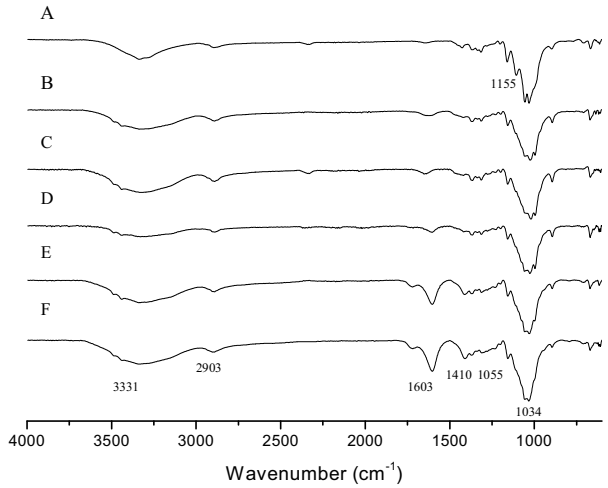

Fig. 1. IR spectra of the initial MCC, mercerized MCC and oxidized MCCs. (A) initial MCC; (B) mercerized MCC; (C) oxidized MCC prepared with 1 mL NaClO solution; (D) oxidized MCC prepared with 5 mL NaClO solution; (E) oxidized MCC prepared with 10 mL NaClO solution; (F) oxidized MCC prepared with 15 mL NaClO solution.

2.2.8. UHPLC-Q/TOF-MS analysis

Each oxidized MCC sample (4 mg) was dissolved in 200 μL distilled water. After vigorous shaking, the suspension was filtered through 0.22 μm microfiltration membrane to remove the undissolved particles. The entire UHPLC-ESI-Q/TOF-MS system was composed of a 1290 UHPLC system (Agilent, CA, USA) and a 6540 Q/TOF-MS, equipped with an Agilent Jet Stream electrospray ion source (Agilent, CA, USA). The sample was subjected to a chromatographic separation with an ACQUITY UPLC@BEH125 SEC column (1.7 μm, 4.6 × 300 mm, Waters, USA) before MS analysis. The chromatographic conditions are as below: mobile phase, 50 mM ammonium acetate aqueous solution (80%), methanol (20%); flow rate, 0.1 mL/min; wavelength, 210 nm; injection volume, 5 μL; column temperature, 25 °C. The MS spectra were obtained in negative mode with a scan range 100 ~ 3000 *m*/*z*. The major MS parameters are as follows: temperature of drying gas, 350 °C; flow rate of drying gas, 8 L/min; pressure of nebulizer, 40 psig; capillary voltage, 3500 v; fragmentor voltage, 120 v (Hao, Lu, Xu, Linhardt, & Zhang, 2016). The data were processed with MassHunter 6.0.

3. Results and discussion

The amount of oxidant has been previously reported to have the most important factor to have impact on the DO of starch (Hao, Lu, Xu, Linhardt, & Zhang, 2016). Thus, in the current study different amounts of oxidant were used in the reactions to produce oxidized MCCs with different DOs.

3.1. Detection of degree of oxidation with IR spectroscopy

The IR spectra of initial, mercerized, and oxidized MCCs prepared with different amounts of oxidant (NaClO solution, 1, 5, 10, 15 mL, 5% active chlorine) are shown in Fig. 1A–F. In the spectrum of initial MCC, the broad absorption band at ~3300 cm^{-1} and the slight band at ~2900 cm^{-1} can be assigned as the stretching vibration of —OH and —CH/—CH_2 groups on the sugar ring, respectively (Gomez-Bujedo, Fleury, & Vignon, 2004; Li et al., 2013). In region between 1500 and 1300 cm^{-1}, the absorption peaks were assigned as multiple vibration modes including —CH (—CH and —CH_2 groups) and —OH bending. The strong bands in the range of 1200–1000 cm^{-1} were assigned as the stretching vibration of C—O from —CH—OH and —CH_2—OH of the sugar ring. All of the spectra in this Figure were normalized against the intensity of the peak at ~3300 cm^{-1} in Fig. 1A. In Fig. 1B, the IR spectrum of mercerized MCC exhibited the similar profile but exhibited slight differences in fingerprint region compared to that of the initial MCC in Fig. 1A. The spectra of the oxidized MCC (Fig. 1C–F) carried out with different amounts of oxidant (NaClO solution, 1, 5, 10 and 15 mL, 5% active chlorine) were similar, except that a new strong and narrow absorption band at ~1600 cm^{-1} appeared in Fig. 1C and became stronger from Fig. 1C–F. This band is attributed to the C=O stretching vibration of carboxyl group (Gomez-Bujedo, Fleury, & Vignon, 2004). The intensity increase of this signal in the spectra of oxidized MCC demonstrates that the larger the amounts of oxidant applied, the greater the formation of carboxyl groups. The bands in the range of 1200–1000 cm^{-1} (Fig. 1C–F) confirm the maintenance of the sugar ring after oxidation.

3.2. Detection of degree of oxidation with solid state ^{13}C NMR spectroscopy

The solid-state ^{13}C NMR spectra of initial, mercerized, and the oxidized MCCs prepared with different amounts of oxidant (1, 5, 10 and 15 mL NaClO solution, 5% active chlorine) are shown in Fig. 2A–F. In the spectrum of initial MCC (Fig. 2A), the singlet at 105.0 ppm was assigned to the anomeric carbon of the glucose residue (Glc, C1). The chemical shifts of C2, C3 and C5 partially overlap in the range of 70–75 ppm as the resolution of solid state NMR is relatively low (Kono, Yunoki, Shikano, Fujiwara, Erata, & Takai, 2002; Saito, Shibata, Isogai, Suguri, & Sumikawa, 2005; Hirota, Tamura, Saito, & Isogai, 2009). The peaks, observed at 88.8 and 84.4 ppm, were assigned to C4 of glucose (Glc, C4) in the crystal and noncrystal structures, respectively (Saito, Shibata, Isogai, Suguri, & Sumikawa, 2005). The peaks, observed at 65.0 and 62.3 ppm, were assigned C6 of glucose (Glc, C6) in the crystal and non-crystal structures, respectively (Saito, Shibata, Isogai, Suguri, & Sumikawa, 2005). As previously reported, the unique resonances of C1, C4 and C6 of MCC observed in ^{13}C NMR spectra indicated the crystalline structure I of cellulose (Saito, Shibata, Isogai, Suguri, & Sumikawa, 2005; Keshk, 2015). The carbon resonance positions of mercerized MCC were similar to those in initial MCC (Fig. 2B). However, the peaks of C1 at ~105.0 ppm and C4 at ~88.8 ppm in the spectrum of mercerized MCC were split, and the peaks of C4 at ~84.4 ppm and C6 at ~65.0 ppm disappeared compared to those in the spectrum of initial MCC. This indicates that the crystalline structure of MCC was affected by mercerization. The spectra of oxidized MCC are shown in Fig. 2C–F. The intensity of the peak at 62.5 ppm, assigned as C6 of glucose (Glc, C6), decreased, while the intensity of the peak at 174.9 ppm, assigned as C6 of glucuronic acid (GlcA, C6), increased from top to bottom spectrum in Fig. 2C–F. These results clearly demonstrate that the larger the amount of oxidant, the greater the conversion of Glc to GlcA, and the higher DO in the selectively oxidized MCC.

3.3. X-ray diffraction (XRD) analysis

The XRD patterns of initial MCC, mercerized MCC and oxidized MCCs are shown in Supplementary data (sFig. 1 A-F). The initial MCC (sFig. 1A) exhibits three diffractions at 2θ = 14.7°, 22.4° and 34.2° in Fig. 3A, which belong to the crystalline structure I of cellulose (Isogai & Atalla, 1998; Saito & Isogai, 2004). The mercerized MCC exhibits three diffractions at 2θ = 11.9°, 19.8° and 21.6° (sFig. 1B) that belong to the crystalline structure II of cellulose (Isogai & Atalla, 1998). The profiles of spectra of oxidized MCC (sFig. 1C–F) are same to that of mercerized MCC, but the greater the oxidant the greater the reduction of the intensity of these diffractions, the greater the reduction of the intensity of these diffractions.

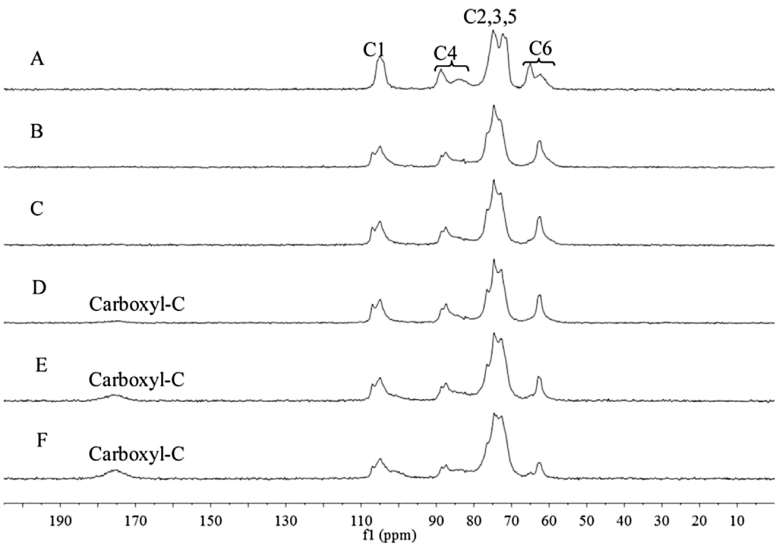

Fig. 2. Solid state ^{13}C NMR spectra of initial MCC, mercerized MCC and oxidized MCCs. (A) initial MCC; (B) mercerized MCC; (C) oxidized MCC prepared with 1 mL NaClO solution; (D) oxidized MCC prepared with 5 mL NaClO solution; (E) oxidized MCC prepared with 10 mL NaClO solution; (F) oxidized MCC prepared with 15 mL NaClO solution.

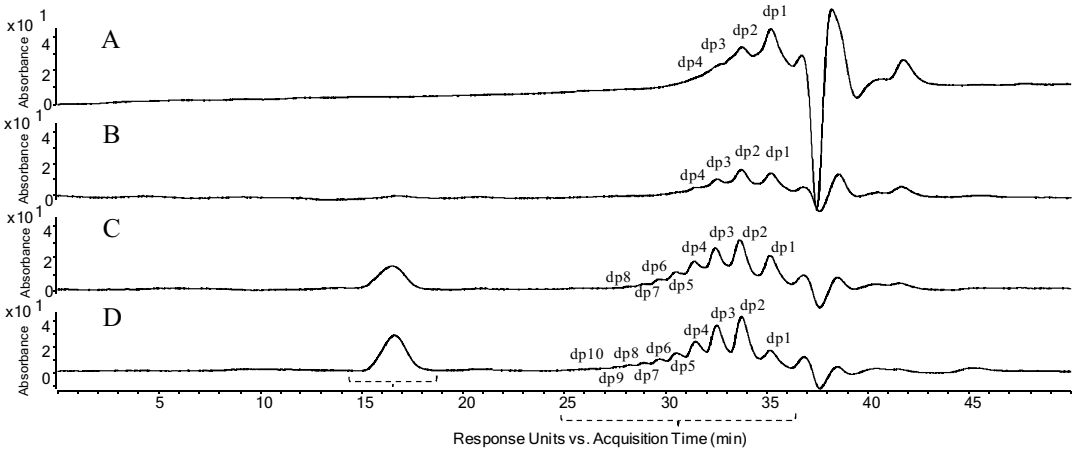

Fig. 3. Size-exclusion chromatograms of oxidized oligosaccharides (A) oxidized MCC prepared with 1 mL NaClO solution; (B) oxidized MCC prepared with 5 mL NaClO solution; (C) oxidized MCC prepared with 10 mL NaClO solution; (D) oxidized MCC prepared with 15 mL NaClO solution.

Thus, the alkaline solution used in mercerization changed the MCC crystalline structure from I to II, and the carboxyl groups formed during the oxidation destroys the highly ordered inter-molecular and intra-molecular hydrogen bonds and even the lattice in MCC crystalline structure.

3.4. Thermal stability of the oxidized mercerized MCC with different DOs

The thermal stability of initial, mercerized and oxidized MCCs were investigated with TGA assays. The results are shown in Supplementary data (sFig. 2). The percentage of weight lost was plotted as a function of temperature. The weight of initial MCC did not drop significantly until 330 °C. However, the weight of mercerized MCC dropped 10% at ~230 °C and dropped sharply at 312 °C. These results indicate that initial MCC had better thermal stability than freshly mercerized MCC. Thus, the highly ordered crystalline structure I of MCC was more stable. The weight of oxidized MCC started to drop at much lower temperature, but the weight dropped gradually. This result demonstrates that the amorphous structures of fully and/or partially oxidized domains in the sugar chains have different thermal stability properties.

3.5. Water solubility of the oxidized mercerized MCC with different DOs

The water solubility of initial, mercerized and oxidized MCC with different DOs are listed in Table 1. The initial MCC could not be dissolved in water but the solubility of the mercerized MCC was about 4%. The solubility of MCC could be significantly increased, from ~10% to ~88%, by selective oxidation, and the higher the DO, the higher the water solubility.

3.6. Molecular weight analysis of dissolved portion from the oxidized MCC

The dissolved portion of oxidized MCC was next analyzed using GPC-MALLS. The molecular weights are listed in Table 2. The MW of dissolved portion of the sample produced with 1 mL oxidant (NaClO solution, 5% active chlorine) was quite low (9.3 kDa). This indi-

Table 1
Aqueous solubility of initial, mercerized and oxidized MCCs (n = 3).

Samples	Water solubility(%)
Initial MCC	0
Mercerized MCC	4.4 ± 0.5
Oxi-MCC-1	10.2 ± 0.3
Oxi-MCC-5	42.8 ± 1.2
Oxi-MCC-10	83.7 ± 4.3
Oxi-MCC-15	87.6 ± 3.0

Oxi- MCC-1 refers to oxidized MCC prepared with 1 mL NaClO solution.
Oxi-MCC-5 refers to oxidized MCC prepared with 5 mL NaClO solution.
Oxi-MCC-10 refers to oxidized MCC prepared with 10 mL NaClO solution.
Oxi-MCC-15 refers to oxidized MCC prepared with 15 mL NaClO solution.

Table 2
Weight-average molecular weight of oxidized MCCs.

Samples	Mw(kDa)	Polydispersity
Oxi-MCC-1	9.3 ± 3.6%	2.8
Oxi-MCC-5	37.8 ± 1.6%	2.7
Oxi-MCC-10	83.5 ± 1.1%	2.9
Oxi-MCC-15	16.1 ± 1.1%	2.8

Oxi-MCC-1 refers to oxidized MCC prepared with 1 mL NaClO solution.
Oxi-MCC-5 refers to oxidized MCC prepared with 5 mL NaClO solution.
Oxi-MCC-10 refers to oxidized MCC prepared with 10 mL NaClO solution.
Oxi-MCC-15 refers to oxidized MCC prepared with 15 mL NaClO solution.

cates that sugar chains with low molecular weight in mercerized MCC could be oxidized easier and faster than other portions of the polysaccharide, and dissolved in water afterwards. The dissolved portion of the samples with higher DOs, such as the MCC oxidized with 5 and 10 mL oxidant (NaClO solution, 5% active chlorine), has significantly higher molecular weights (37.8 and 83.5, respectively). This result indicates that longer sugar chains in mercerized MCC have a greater chance to be oxidized and then dissolved into water when the MCC was exposed to higher concentrations of oxidant solution. Interestingly, the molecular weight of the oxidized MCC with the highest DO was 16.1 kDa and we speculate that the oxidation degraded these sugar chains. Furthermore, the additional 5 mL oxidant was added to Oxi-MCC-10. The oxidation was carried out at 50 °C for 2 h with same conditions. The solubility of re-oxidized MCC (Oxi-MCC–10 + 5) did not change much, (~86%) but its molecular weight dropped from ~84 kD to ~28 kD. Thus, it is confirmed that oxidation degrades MCC.

3.7. Structural analysis of dissolved portion from the oxidized MCC

A detailed structure analysis of the dissolved products provides a deeper insight into the physicochemical properties of the oxidized MCC. The chromatograms of the dissolved products of the oxidized MCCs, detected at 210 nm are presented in Fig. 3. Some peaks corresponding to oligosaccharides were observed. Their molecular weight and degree of polymerization (dp) were confirmed by MS spectrometry (Fig. 4). Small oligosaccharides, dp1-dp4, were observed in the products oxidized with 1 mL oxidant (5% active chlorine) in Fig. 3A. The content of dp1 and 2 decreased and the content of dp3 and 4 relatively increased in Fig. 3B. Larger oligosaccharides and a broad peak corresponding to polysaccharide are observed in Fig. 3C and D.

In the MS spectra, the molecular ions, observed as either singly charged or doubly charged ions are labeled with subscript "1" or "2" adjacent to the corresponding dp number. In Fig. 4A, three ions observed at *m*/*z* 209, 179 and 149, were assigned as three types of oxidized glucuronic acid (GlcA). These assignments are listed in Table 3 and their structures are shown in Scheme 1. After the glycosidic bonds are oxidatively cleaved, the resulting hemiacetal groups

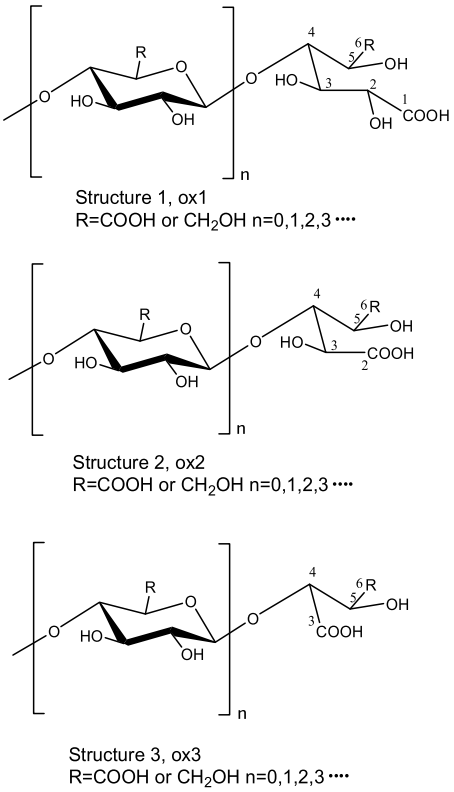

Scheme 1. Different structural forms of oxidized MCC oligosaccharides.

at the reducing end of sugar residues are then further oxidized to carboxyl group at the position 1 and the ring opened. (Structure 1, ox1 form) The oxidation does not stop after the reducing end C1 is oxidized to carboxyl group but further oxidation can take place under these conditions (Hao, Lu, Xu, Linhardt, & Zhang, 2016). The bond linking C1 and C2 in the reducing end residue is cleaved, and position 2 was oxidized to carboxyl group to form the Structure 2. Furthermore, the bond linked C2 and C3 in the reducing end residue was cleaved and position 3 was oxidized to carboxyl group to form the Structure 3. These three structural forms were observed in each dp and their assignments are listed in Table 3. Oligosaccharides with different DOs were observed in the products oxidized with 1 mL oxidant, including disaccharides with one and two GlcA residues in three structural forms. The molecular ions corresponding to trisaccharides and tetrasaccharides with different compositions (number of Glc or GlcA) and structural forms (ox1 ox2 and ox3) are also observed in the MS spectra (not shown) and listed in Table 3. The fully oxidized oligosaccharides in three structural forms are observed in the products oxidized with 5–15 mL oxidant. The MS spectra of fully oxidized dp2-dp6 are presented in Fig. 4B–F. In addition, when higher oxidant levels were applied, less the oligosaccharides in structural form 1 were produced and more the oligosaccharides in structural forms 2 and 3 were obtained.

4. Discussion and conclusion

The amount of oxidant is the most important factor impacting the DO when a polysaccharide is oxidized with the TEMPO–NaBr–NaClO system (Hao, Lu, Xu, Linhardt, & Zhang, 2016). In current study, the oxidized MCC with different DOs were prepared using different amounts of oxidant. IR and solid-state ^{13}C NMR were used to confirm the crystalline structures of initial MCC,

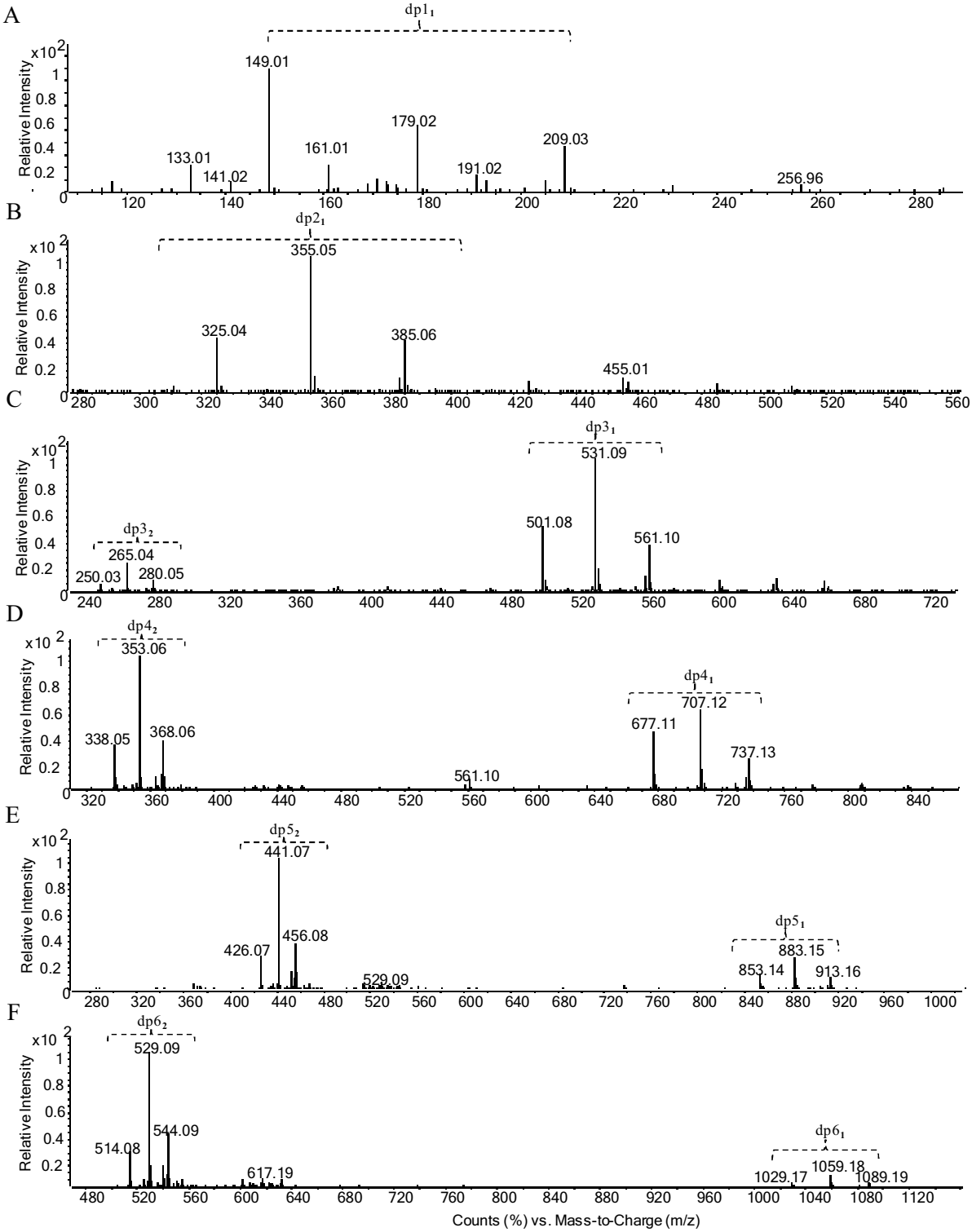

Fig. 4. MS spectra of fully oxidized oligosaccharides (dp1-dp6) (A) MS spectrum of full oxidized dp1; (B) MS spectrum of full oxidized dp2; (C) MS spectrum of full oxidized dp3; (D) MS spectrum of full oxidized dp4; (E) MS spectrum of full oxidized dp5; (F) MS spectrum of full oxidized dp6.

mercerized MCC, and DO trend of the oxidized MCC. The crystalline structure of MCC and mercerized MCC were also confirmed with XRD. The crystalline structure I of MCC could be converted into crystalline structure II by fresh mercerization with alkaline solution. Furthermore, the carboxyl groups selectively prepared at the C6 position on the sugar ring using TEMPO oxidation disrupted the

Table 3
MS Assignments of the oligosaccharides degraded from oxidized MCCs.

Degree of polymerization	Structures	*m/z*	Relative Intensity (%) at each dp			
			1 mL	5 mL	10 mL	15 mL
dp 1	$(Glc)_{ox1}$	195	22	–	–	–
	$(GlcA)_{ox1}$	209	43	100	100	38
	$(GlcA)_{ox2}$	179	100	93	90	55
	$(GlcA)_{ox3}$	149	71	80	88	100
dp 2	$(GlcGlcA)_{ox1}$	371	23	–	–	–
	$(GlcGlcA)_{ox2}$	341	19	–	–	–
	$(GlcGlcA)_{ox3}$	311	9	–	–	–
	$(GlcA_2)_{ox1}$	385	100	79	36	3
	$(GlcA_2)_{ox2}$	355	99	100	100	100
	$(GlcA_2)_{ox3}$	325	94	61	40	49
dp 3	$(GlcGlcA_2)_{ox1}$	547	100	–	–	–
	$(GlcGlcA_2)_{ox2}$	517	88	–	–	–
	$(GlcGlcA_2)_{ox3}$	487	84	–	–	–
	$(GlcA_3)_{ox1}$	561	88	72	34	3
	$(GlcA_3)_{ox2}$	531	88	100	100	100
	$(GlcA_3)_{ox3}$	501	76	56	47	52
dp 4	$(Glc_2GlcA_2)_{ox1}$	709	100	–	–	–
	$(Glc_2GlcA_2)_{ox2}$	679	95	–	–	–
	$(Glc_2GlcA_2)_{ox3}$	649	76	–	–	–
	$(GlcGlcA_3)_{ox1}$	723	62	–	–	–
	$(GlcGlcA_3)_{ox2}$	693	62	–	–	–
	$(GlcGlcA_3)_{ox3}$	663	52	–	–	–
	$(GlcA_4)_{ox1}$	737	–	69	35	6
	$(GlcA_4)_{ox2}$	707	–	100	100	100
	$(GlcA_4)_{ox3}$	677	–	46	43	49
dp 5	$(GlcGlcA_4)_{ox1}$	899	100	–	–	–
	$(GlcGlcA_4)_{ox2}$	869	93	–	–	–
	$(GlcGlcA_4)_{ox3}$	839	43	–	–	–
	$(GlcA_5)_{ox1}$	913	73	72	35	8
	$(GlcA_5)_{ox2}$	883	70	100	100	100
	$(GlcA_5)_{ox3}$	853	30	34	34	39
dp 6	$(Glc_3GlcA_3)_{ox1}$	1047	67	–	–	–
	$(Glc_3GlcA_3)_{ox2}$	1017	52	–	–	–
	$(Glc_3GlcA_3)_{ox3}$	987	29	–	–	–
	$(Glc_2GlcA_4)_{ox1}$	1061	100	–	–	–
	$(Glc_2GlcA_4)_{ox2}$	1031	76	–	–	–
	$(Glc_2GlcA_4)_{ox3}$	1001	48	–	–	–
	$(GlcGlcA_5)_{ox1}$	1075	–	–	–	–
	$(GlcGlcA_5)_{ox2}$	1045	–	–	–	–
	$(GlcGlcA_5)_{ox3}$	1015	–	–	–	–
	$(GlcA_6)_{ox1}$	1089	–	75	38	11
	$(GlcA_6)_{ox2}$	1059	–	100	100	100
	$(GlcA_6)_{ox3}$	1029	–	25	30	33

"-" not detected.

crystalline structure II of mercerized MCC, and the greater the number of carboxyl groups formed, the lower the level of crystalline structure II remained in mercerized MCC. Accordingly, the solubility of MCC increased from 0%, to about 4%, following mercerization, to about 88%, following a high level of oxidation of MCC.

The dissolved portion of each oxidized MCC was characterized with GPC-MALLS and UHPLC-Q/TOF-MS. The molecular weight of the dissolved portion in the oxidized MCC with low DO was low, indicating that the sugar chains with low molecular weight in mercerized MCC was easier to oxidize and dissolve in water when a limited amount of oxidant was applied. The molecular weights of dissolved portion of oxidized MCCs increased to ~38 kD and ~84 kD, when 5 and 10 mL NaClO solution (5% active chlorine) were applied, respectively. These results indicate that the longer sugar chains oxidize and dissolve into water when a higher amount of oxidant was applied. The relatively low molecular weight (~16 kD) of the highly oxidized MCC suggests that degradation takes place during the oxidation of MCC. Furthermore, the results observed in LC–MS analytical data confirm that degradation was always coupled with oxidation. Small oxidized and partially oxidized oligosaccharides (dp1-dp4) were observed in the products produced with 1 mL oxidant (NaClO solution, 5% active chlorine), which are degraded from short and partially oxidized sugar chains. Bigger and fully oxidized oligosaccharides were observed in the products produced with higher amount of oxidant (5–15 mL NaClO solution, 5% active chlorine), which are degraded from longer and oxidized sugar chains. In addition, there were three structural forms in the MCC oxidation products, which are derivatives of the oxidized oligosaccharides.

Thus, we conclude that the degree of oxidation of MCC affects its crystalline structure, solubility, thermal stability, molecular weight and the structures of degraded products. These physiochemical properties should support many potential new applications of oxidized MCC.

Acknowledgements

The work was supported by the National Natural Science Foundation of China (81473179, 81673388), Priority Academic Program Development of Jiangsu Higher Education Institutions (PAPD, YX13200111), and the funding for Jiangsu Key Laboratory

of Translational Research and Therapy for Neuro-Psycho-Diseases (BM2013003).

Appendix A. Supplementary data

Supplementary data associated with this article can be found, in the online version, at http://dx.doi.org/10.1016/j.carbpol.2016.09.012.

References

Assa, B. A. P., Belgacemb, M. N., & Frollinia, E. (2006). Mercerized linters cellulose: Characterization and acetylation in N,N-dimethylacetamide/lithium chloride. *Carbohydrate Polymers*, *63*, 19–29.

Benchabane, A., & Bekkour, K. (2008). Rheological properties of carboxymethyl cellulose (CMC) solutions. *Colloid and Polymer Science*, *286*, 1173–1180.

Benhamou, K., Dufresne, A., Magnin, A., Mortha, G., & Kaddami, H. (2014). Control of size and viscoelastic properties of nanofibrillated cellulose from palm tree by varying the TEMPO-mediated oxidation time. *Carbohydrate Polymers*, *99*, 74–83.

Bochek, A., Petropavlovsky, G., & Kallistov, O. V. (1993). Dissolution of cellulose and its derivatives in the same solvent: Methylmorpholine-*N*-oxide and the properties of the resulting solutions. *Cellulose Chemistry and Technology*, *27*, 137–144.

Gomez-Bujedo, S., Fleury, E., & Vignon, M. R. (2004). Preparation of cellouronic acids and partially acetylated cellouronic acids by TEMPO/NaClO oxidation of water-soluble cellulose acetate. *Biomacromolecules*, *5*, 565–571.

Guo, W., & Ruckenstein, E. (2002). Crosslinked mercerized cellulose membranes for the affinity chromatography of papain inhibitors. *Journal of Membrane Science*, *197*, 53–62.

Gurgel, L. V. A., Melo, J. C. P., Lena, J. C., & Gil l, F. (2009). Adsorption of chromium (VI) ion from aqueous solution by succinylated mercerized cellulose functionalized with quaternary ammonium groups. *Bioresource Technology*, *100*, 3214–3220.

Hao, J., Lu, J. J., Xu, N. Y., Linhardt, R. J., & Zhang, Z. Q. (2016). Specific oxidation pattern of soluble starch with TEMPO-NaBr-NaClO system. *Carbohydrate Polymers*, *146*, 238–244.

Hirota, M., Tamura, N., Saito, T., & Isogai, A. (2009). Oxidation of regenerated cellulose with $NaClO_2$ catalyzed by TEMPO and NaClO under acid-neutral conditions. *Carbohydrate Polymers*, *78*, 330–335.

Huang, C. F., Chen, J. K., Tsai, T. Y., Hsieh, Y. A., & Andrew Lin, K. Y. (2015). Dual-functionalized cellulose nanofibrils prepared through TEMPO mediated oxidation and surface-initiated ATRP*. *Polymer*, *72*, 395–405.

Isogai, A., & Atalla, R. H. (1998). Dissolution of cellulose in aqueous NaOH solutions. *Cellulose*, *5*, 309–319.

Isogai, A., & Kato, Y. (1998). Preparation of polyuronic acid from cellulose by TEMPO-mediated oxidation. *Cellulose*, *5*, 153–164.

Jackson, E. L., & Hudson, C. S. (1937). Application of the cleavage type of oxidation by periodic acid to starch and cellulose. *Journal of the American Chemical Society*, *59*, 2049–2050.

Keshk, S. M. A. S. (2015). Effect of different alkaline solutions on crystalline structure of cellulose at different temperatures. *Carbohydrate Polymers*, *115*, 658–662.

Klemm, D., Philip, B., Heinz, T., Heinz, U., & Wagenknecht, W. (1998). . pp. 9–25. *Comprehensive cellulose chemistry* (vol. 1) Weinheim: Wiley-VCH.

Kono, H., Yunoki, S., Shikano, T., Fujiwara, M., Erata, T., & Takai, M. (2002). CP/MAS ^{13}C NMR study of cellulose and cellulose derivatives: 1. complete assignment of the CP/MAS ^{13}C NMR spectrum of the native cellulose. *Journal of the American Chemical Society*, *124*, 7506–7511.

Kono, H., Oshima, K., Hashimoto, H., Shimizu, Y., & Tajima, K. (2016). NMR characterization of sodium carboxymethyl cellulose: Substituent distribution and mole fraction of monomers in the polymer chains. *Carbohydrate Polymers*, *146*, 1–9.

Li, L., Zhao, S., Zhang, J., Zhang, Z. X., Hu, H. Q., Xin, Z. X., et al. (2013). TEMPO-mediated oxidation of microcrystalline cellulose: Influence of temperature and oxidation procedure on yields of water-soluble products and crystal structures of water-insoluble residues. *Fibers and Polymers*, *14*, 352–357.

Li, B., Xu, W. Y., Kronlund, D., Määttänen, A., Liu, J., Smått, J. H., et al. (2015). Cellulose nanocrystals prepared via formic acid hydrolysis followed by TEMPO-mediated oxidation. *Carbohydrate Polymers*, *133*, 605–612.

Qin, X. Z., Lu, A., Cai, J., & Zhang, L. (2013). Stability of inclusion complex formed by cellulose in NaOH/urea aqueous solution at low temperature. *Carbohydrate Polymers*, *92*, 1315–1320.

Saito, T., & Isogai, A. (2004). TEMPO-Mediated oxidation of native cellulose: The effect of oxidation conditions on chemical and crystal structures of the water-Insoluble fractions. *Biomacromolecules*, *5*, 1983–1989.

Saito, T., Shibata, I., Isogai, A., Suguri, N., & Sumikawa, N. (2005). Distribution of carboxylate groups introduced into cotton linters by the TEMPO-mediated oxidation. *Carbohydrate Polymers*, *61*, 414–419.

Shinoda, R., Saito, T., Okita, Y., & Isogai, A. (2012). Relationship between length and degree of polymerization of TEMPO-Oxidized cellulose nanofibrils. *Biomacromolecules*, *13*, 842–849.

Siller, M., Amer, H., Bacher, M., Roggenstein, W., Rosenau, T., & Potthast, A. (2015). Effects of periodate oxidation on cellulose polymorphs. *Cellulose*, *22*, 2245–2261.

Sirvio, J., Hyvakko, U., Liimatainen, H., Niinimaki, J., & Hormi, O. (2011). Periodate oxidation of cellulose at elevated temperatures using metal salts as cellulose activators. *Carbohydrate Polymers*, *83*, 1293–1297.

Suhas, Gupta, V. K., Carrott, P. J. M., Singh, R., Chaudhary, M., & Kushwaha, S. (2016). Cellulose: A review as natural: Modified and activated carbon adsorbent. *Bioresource Technology*, *216*, 1066–1076.

Tahiri, C., & Vignon, M. (2000). TEMPO-oxidation of cellulose: Synthesis and characterisation of polyglucuronans. *Cellulose*, *7*, 177–188.

Ugwoke, M. I., Kaufmann, G., Verbeke, N., & Kinget, R. (2000). Intranasal bioavailability of apomorphine from carboxymethylcellulose-based drug delivery systems. *International Journal of Pharmaceutics*, *202*, 125–131.